

# Partially Distributed Multirobot Control with Multiple Cameras

M. Aranda, Y. Mezouar, G. López-Nicolás and C. Sagüés

**Abstract**—We present a new method for visual control of a set of robots moving on the ground plane. As contributions, we first propose a purely image-based control strategy that drives the set to a desired configuration while minimizing at all times the sum of the squared distances the robots have to travel. This homography-based method, which has low computational cost and generates smooth trajectories for the robots, is then used in a multirobot control framework featuring multiple cameras, each of them observing a subset of the robot team. In particular, we present a novel control approach that makes the complete robot set reach its global target configuration when there exists partial overlap between the subsets of robots observed by the different cameras. Each camera is associated to a control unit which sends the control commands to its observed subset of robots, but no other communication is required between the robots or control units. Our method, which overcomes the field-of-view limitations of single-camera methods and increases their scalability, exploits the advantages of both centralized and distributed multirobot control strategies. Simulations are provided to illustrate the performance of the proposal.

## I. INTRODUCTION

Multirobot systems have been a very popular research topic in recent years, as they allow to perform a number of tasks with higher efficiency than a single robot. This work addresses in particular the control of a group of ground mobile robots, a field where a variety of setups and objective tasks have been considered (leader-follower behavior [1], [2], formation control [3], [4], rendezvous [5]). Regarding the type of sensing employed, the rich information provided by vision has led to its use in a number of approaches within the topic of multirobot motion control [6]–[10]. In general, control strategies such as the cited ones can be classified into two main types: centralized or distributed, each of the two categories having well-known pros and cons.

In the field of visual control [11], multiple view geometric models have proven to be a valuable tool that allows to enhance the robustness of performance. However, the use of these models for multirobot control tasks has rarely been explored. In this paper, we propose a method that uses the homography model (which has been widely employed for the control of a single mobile robot [12]–[14]) in a multirobot scenario. In particular, the homography computed between the current and target images of the group of robots is used to

obtain their motion control commands. We tackle the task of bringing a set of mobile robots from arbitrary initial positions to a desired geometric configuration.

The approach presented in this article originates from a method introduced in [15], which was extended in [16]. In this previous work, we proposed a visual control framework based on homography to drive a group of robots to a desired configuration. Taking advantage of the geometry of the framework (i.e. planar motion of the robots and the flying camera system), the control relied on the definition of a desired homography, computed from the projections of the robots in a reference image and in the current image, and satisfying a particular parametrization. Some advantages of the preceding approaches [15], [16] which are maintained in the present work, are that the camera can move arbitrarily without affecting the control performance, and the behavior of the complete robot set is handled by one single homography, computed efficiently by solving a linear system.

However, in this work we approach the control problem from a different perspective. Motivated by the objective of improving the motion of the robots, we propose a method that minimizes the sum of squared distances between the robots' current and desired positions on the plane to reach the desired configuration. Notably, we achieve this goal with a purely image-based method, not requiring any explicit pose computation. Like the previous works did, we employ a desired homography to define the control objective in the image plane. However, the procedure we propose to determine this objective is different, and it requires a homography defined with fewer parameters. The advantages of the new proposal are that the trajectories are shorter than in the preceding ones, and the load of the control task is shared more equitably among the robots. In addition, the computational cost is lower, thanks to the reduced homography parametrization.

Furthermore, and contrary to our earlier works, the approach we present in this paper is designed to be used in a multi-camera scenario. Indeed, we propose a partially distributed scheme where the robots are controlled cooperatively through multiple cameras, each of which observing a subset of the robot team. Each camera is fixed to a control unit (a mobile robot), which applies the proposed control technique to the subset of robots within the camera's field of view. We show that if a minimum overlap of two robots exists among the subsets, the controllers have implicit coordination and perform the desired task (i.e. reach the target configuration) for the full set of robots cooperatively. Thus, this approach has the advantage of not requiring any communication between the control units. The fact that the control units can move arbitrarily is another important

M. Aranda, G. López-Nicolás and C. Sagüés are with Instituto de Investigación en Ingeniería de Aragón, Universidad de Zaragoza, Spain. {marandac, gonlopez, csagues}@unizar.es

Y. Mezouar is with Clermont Université, IFMA, Institut Pascal, Clermont-Ferrand, France. youcef.mezouar@ifma.fr

This work was supported by Ministerio de Ciencia e Innovación/European Union (projects DPI2009-08126 and DPI2012-32100), Ministerio de Educación under FPU grant AP2009-3430, DGA-FSE (group T04), French ANR projects ARMEN (ANR-09-TECS-020) and the LabEx IMobS3 (ANR-10-LABX-16-01).

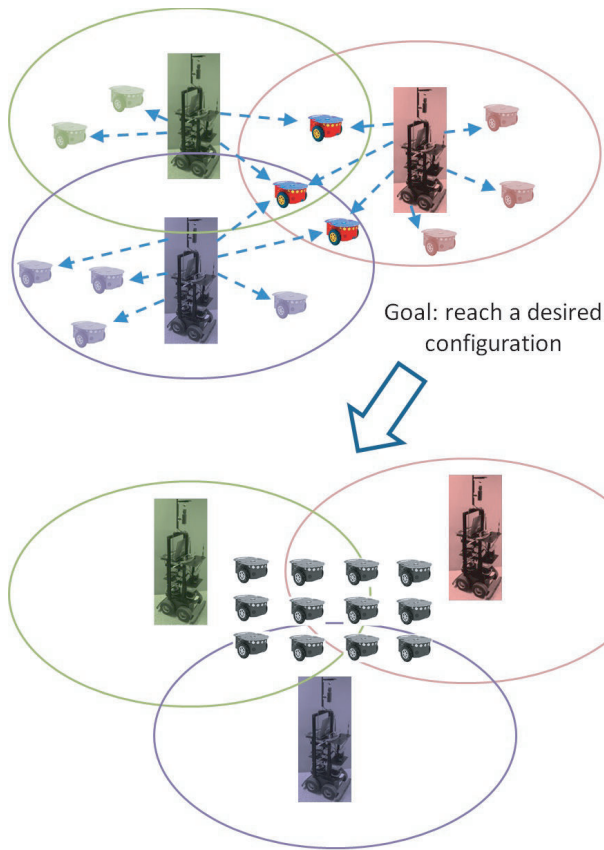


Fig. 1. Overview of the proposed system for multirobot control. Multiple (three, in this example) control units are used. Each of them has an associated camera from which the unit obtains, using the proposed homography-based approach, the motion commands for all the robots within the camera's field of view (represented by an ellipse). These velocities are transmitted to the controlled robots, each of which selects from all the commands it receives the one having minimum absolute linear velocity. The control units can move arbitrarily, and no communication occurs between them.

advantage, since this means their motion can be selected in order to optimize the visibility of the robots, guarantee the required overlaps between subsets, etc.

The application scenario we consider for the multi-camera technique proposed is one where the control task is handled by a number of control units, each of them consisting of a ground robot carrying a calibrated omnidirectional camera. The proposed setup, illustrated in Fig. 1, allows to bring the robots to a desired rendezvous configuration, which can be useful for exploration, surveillance or rescue tasks.

## II. HOMOGRAPHY-BASED FRAMEWORK

This section describes the characteristics of our framework and how the desired homography is computed. The next section will discuss how this homography is used by the control units to drive a set of robots to a desired configuration.

Let us define the elements of the technique that is implemented by each of the control units depicted in Fig. 1. We consider a number of unicycle robots lying on the ground plane, being observed by a camera with its image plane parallel to the ground at constant height. The control unit associated to the camera has the information of the desired

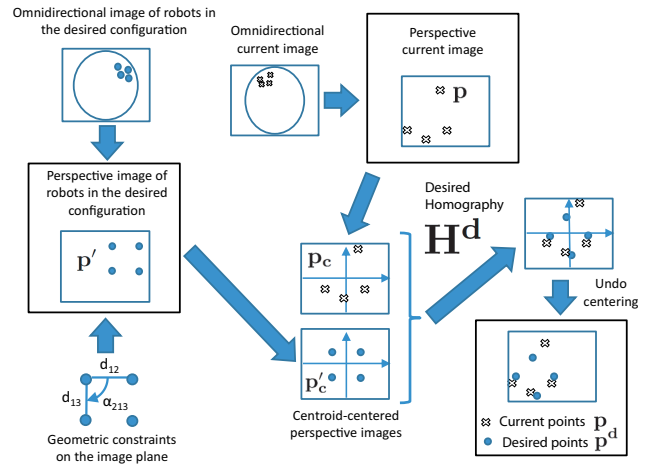


Fig. 2. Overview of the homography-based framework implemented by each of the control units using its associated camera. The desired configuration is given either as an image (perspective or omnidirectional) or as a set of geometrical constraints between the locations of the robots. Throughout the definition of our homography-based method, we use two images of the robot set (the image of the desired configuration and the current image) and we consider them to be perspective. Note, however, that omnidirectional images can equivalently be used with our approach, since they can be converted to perspective images if the calibration is known. In addition, if the desired configuration is given in the form of geometrical constraints, these can also be expressed in the image plane (and can therefore be used in our proposal) with the knowledge of the calibration and height of the camera. A graphical depiction of this process and of the homography-based framework described throughout this section is provided in Fig. 2.

configuration of its viewed robots, either as an image of the robots in that configuration or as a set of geometrical constraints between the locations of the robots. Throughout the definition of our homography-based method, we use two images of the robot set (the image of the desired configuration and the current image) and we consider them to be perspective. Note, however, that omnidirectional images can equivalently be used with our approach, since they can be converted to perspective images if the calibration is known. In addition, if the desired configuration is given in the form of geometrical constraints, these can also be expressed in the image plane (and can therefore be used in our proposal) with the knowledge of the calibration and height of the camera. A graphical depiction of this process and of the homography-based framework described throughout this section is provided in Fig. 2.

We assume the robots can be detected and identified in the images. Each robot is associated with an image point, given by the geometrical center of its projection in the camera image. We define  $\mathbf{p}' = \{\mathbf{p}'_1, \dots, \mathbf{p}'_n\}$  as the set of points in the image of the desired configuration and  $\mathbf{p}(t) = \{\mathbf{p}_1(t), \dots, \mathbf{p}_n(t)\}$  as the set of points in the current image. That is, robot  $i$  ( $i = 1, \dots, n$ ) is projected in point  $\mathbf{p}'_i$  in the image of the desired configuration and in point  $\mathbf{p}_i(t)$  in the current one.

### A. Desired image points to minimize the sum of squared distances

When attempting to improve the characteristics of the motion of a set of robots, there are different metrics that may be considered. In particular, our method minimizes the sum of squared distances between the robots' current and desired positions on the plane to reach the desired configuration.

We start by looking at the relationship between the two sets of points  $\mathbf{p}'$  and  $\mathbf{p}$  defined in the previous section. This relationship depends on the robot and camera motions. In our framework, the image plane is parallel to the plane of the robots, and its height is constant. Thus, the distances between robot projections in the image plane are equivalent to the actual distances between the robots, up to a constant scale factor. In addition, when the robots are in the desired configuration in the current image, the distances between their projections in the current image plane will be the same as in the reference image. This means that it is possible to express the relationship between  $\mathbf{p}'$  and  $\mathbf{p}$  as a projective transformation (or homography) of 2D that preserves the Euclidean distances, i.e. a Euclidean transformation.

When the robots are not in the desired configuration, the two sets of points are not related by a Euclidean transformation. We propose in our method to use the points in correspondence in  $\mathbf{p}'$  and  $\mathbf{p}$  to compute a homography, constrained to be Euclidean. Thus, the data is not compatible with this form of homography. We can, however, solve the system using SVD and obtain a least-squares solution. This desired homography ( $\mathbf{H}^d$ ) defines a mapping (whose details are given in the next section) of  $\mathbf{p}'$  to a new set of points ( $\mathbf{p}^d(t) = \{\mathbf{p}_1^d(t), \dots, \mathbf{p}_n^d(t)\}$ ) in the current image, having this property:

$$\mathbf{p}^d(\mathbf{H}^d, \mathbf{p}', \mathbf{p}) \ni S = \sum_{i=1}^n \|\mathbf{p}_i - \mathbf{p}_i^d\|^2 \text{ is minimum.} \quad (1)$$

Thus, if we use  $\mathbf{p}^d$  as the set of desired positions in the image plane for each of the robots, and we define a control strategy based on driving the projections of the robots in the image plane from  $\mathbf{p}$  to  $\mathbf{p}^d$ , we are effectively driving the robot set to the desired configuration while making the sum of squared distances from the robots' current positions on the ground plane to their target ones minimum.

### B. Desired homography parametrization and computation

Consider first a general Euclidean homography in 2D, that we call  $\mathbf{H}_e$ , which performs a rotation ( $\phi_e$ ) and translation ( $\mathbf{t} = (t_{xe}, t_{ye})^T$ ) of the points:

$$\mathbf{H}_e = \begin{bmatrix} \cos \phi_e & \sin \phi_e & t_{xe} \\ -\sin \phi_e & \cos \phi_e & t_{ye} \\ 0 & 0 & 1 \end{bmatrix}. \quad (2)$$

A homography is always defined up to a scale factor. Thus, a homography with the form of  $\mathbf{H}_e$  has three degrees of freedom. It can be computed linearly from a minimum of two corresponding points. If we compute  $\mathbf{H}_e$  from  $\mathbf{p}'$  and  $\mathbf{p}$  and apply this *rigid* transformation to the set of points in the image of the desired configuration,  $\mathbf{p}'$ , we obtain a new set of points  $\mathbf{p}_e^d$ :

$$\mathbf{p}_e^d = \mathbf{H}_e \cdot \mathbf{p}'. \quad (3)$$

The centroid of a set of points is defined as the point that minimizes the sum of squared Euclidean distances from the

points in the set to it. For a set of  $n$  image points  $\mathbf{p} = \{\mathbf{p}_1, \dots, \mathbf{p}_n\}$ , the centroid can be easily computed as:

$$\mathbf{c}_p = \frac{1}{n} \sum_{i=1}^n \mathbf{p}_i. \quad (4)$$

Now, note that among all the possible Euclidean homographies, we want to choose the one which verifies that the sum of squared distances between the points in the sets  $\mathbf{p}$  and  $\mathbf{p}_e^d$  is minimum. It can be shown that, in order for this to happen, the centroids of the two sets must coincide. As a consequence, we do not need our desired homography to encode any translation parameters. Instead, we translate the coordinates of the sets of points  $\mathbf{p}'$  and  $\mathbf{p}$  so that they are centered on their respective centroids:

$$\mathbf{p}'_c = \mathbf{p}' - \mathbf{c}_{p'}, \quad \mathbf{p}_c = \mathbf{p} - \mathbf{c}_p. \quad (5)$$

This way, the centroids of  $\mathbf{p}'_c$  and  $\mathbf{p}_c$  are equal. Then we compute, using  $\mathbf{p}'_c$  and  $\mathbf{p}_c$ , a Euclidean homography that expresses a pure rotation, with zero translation. Thus, the centroid of the points resulting from this homography mapping will be the same as the centroid of  $\mathbf{p}_c$ . This simplified definition of the desired homography decreases the cost of its computation by reducing the number of degrees of freedom and, consequently, the size of the system to be solved. A purely rotational Euclidean homography has the following form:

$$\mathbf{H}_r = \begin{bmatrix} h_{11}^r & h_{12}^r & 0 \\ h_{21}^r & h_{22}^r & 0 \\ 0 & 0 & h_{33}^r \end{bmatrix} \sim \begin{bmatrix} \cos \phi_r & \sin \phi_r & 0 \\ -\sin \phi_r & \cos \phi_r & 0 \\ 0 & 0 & 1 \end{bmatrix}. \quad (6)$$

We need to constrain the homography to be computed, in such a way that it has the form of  $\mathbf{H}_r$ . Let us then formulate the constraints that define this homography (assuming it has been normalized by the entry  $h_{33}^r$ ):

$$h_{11}^r = h_{22}^r, \quad h_{12}^r = -h_{21}^r, \quad h_{11}^{r^2} + h_{12}^{r^2} = 1. \quad (7)$$

Looking for a linear solution, we use the fact that the first two constraints in (7) are linear. We can then define, incorporating only these two constraints and not the third (nonlinear) one, a parametrization of the homography having the following form:

$$\mathbf{H}_1 = \begin{bmatrix} h_{11}^l & h_{12}^l & 0 \\ -h_{12}^l & h_{11}^l & 0 \\ 0 & 0 & h_{33}^l \end{bmatrix} \sim \begin{bmatrix} s \cos \phi_l & s \sin \phi_l & 0 \\ -s \sin \phi_l & s \cos \phi_l & 0 \\ 0 & 0 & 1 \end{bmatrix}. \quad (8)$$

The homography  $\mathbf{H}_1$  is *nonrigid* and has two degrees of freedom: the angle of rotation  $\phi_l$  and a scale factor  $s$ . Since each point correspondence provides two independent equations,  $\mathbf{H}_1$  can be computed from only one point match, like  $\mathbf{H}_r$ . However, unlike  $\mathbf{H}_r$ ,  $\mathbf{H}_1$  can be obtained linearly.

If we assume the homographies are computed in such a way that they fit the data with least squares error, then solving for (8) gives the same solution for the angle of rotation as solving for (6), as shown next.

*Proposition 1:* Let  $\mathbf{p}'$  and  $\mathbf{p}$  be two sets of  $n$  image points. Let  $\mathbf{H}_r$  be the least-squares homography computed from  $\mathbf{p}'$  and  $\mathbf{p}$  having the form (6), and let  $\mathbf{H}_l$  be the least-squares homography computed from  $\mathbf{p}'$  and  $\mathbf{p}$  having the form (8). Then,  $\mathbf{H}_r = \mathbf{H}_l \cdot \text{diag}(1/s, 1/s, 0)$ .

*Proof:* Let us define  $\mathbf{p}_r^d = \mathbf{H}_r \cdot \mathbf{p}'$ , and the image coordinates of the individual point  $i$  as  $\mathbf{p}_{ri}^d = (p_{rxi}^d, p_{ryi}^d)^T$ ,  $\mathbf{p}_i = (p_{xi}, p_{yi})^T$  and  $\mathbf{p}'_i = (p'_{xi}, p'_{yi})^T$ . Then, the sum of squared Euclidean distances in the image plane between the transformed image points  $\mathbf{p}_r^d$  and the points  $\mathbf{p}$  is given by:

$$S_r = \sum_{i=1}^n \|\mathbf{p}_i - \mathbf{p}_{ri}^d\|^2 = (p'_{xi}{}^2 + p'_{yi}{}^2) + (p_{xi}^2 + p_{yi}^2) - 2[\cos \phi_r (p'_{xi} p_{xi} - p'_{yi} p_{yi}) + \sin \phi_r (p'_{yi} p_{xi} - p'_{xi} p_{yi})]. \quad (9)$$

For  $\mathbf{H}_l$ , we get:  $\mathbf{p}_l^d = \mathbf{H}_l \cdot \mathbf{p}'$ , and the sum of squared distances is:

$$S_l = \sum_{i=1}^n \|\mathbf{p}_i - \mathbf{p}_{li}^d\|^2 = (p'_{xi}{}^2 + p'_{yi}{}^2) + \frac{1}{s} (p_{xi}^2 + p_{yi}^2) - \frac{2}{s} [\cos \phi_l (p'_{xi} p_{xi} - p'_{yi} p_{yi}) + \sin \phi_l (p'_{yi} p_{xi} - p'_{xi} p_{yi})]. \quad (10)$$

Since we find the least-squares solutions to the homography in the two cases, both  $S_r$  and  $S_l$  are minimum. Assuming that  $s$  is a positive scale factor, it can be seen that if a given angle  $\phi_r$  minimizes  $S_r$ , then an angle  $\phi_l$  of the same value minimizes  $S_l$  as well, and viceversa. Therefore,  $\phi_r = \phi_l$ , and  $\mathbf{H}_r = \mathbf{H}_l \cdot \text{diag}(1/s, 1/s, 0)$ . ■

Taking advantage of this proposition, we compute  $\mathbf{H}_l$  from  $\mathbf{p}'_c$  and  $\mathbf{p}_c$  and then we obtain the desired homography, having the required shape (6), as:

$$\mathbf{H}^d = \mathbf{H}_l \cdot \text{diag}(1/s, 1/s, 0), \quad (11)$$

where  $s$  is computed as the norm of the upper left hand  $2 \times 2$  matrix of  $\mathbf{H}_l$ .

Note that after we compute the desired homography ( $\mathbf{H}^d$ ), the image positions given by the mapping it encodes must be translated back so that they are centered on the actual centroid of the points in the current image. That is, the desired image points are obtained as follows:

$$\mathbf{p}^d = \mathbf{H}^d \mathbf{p}'_c + \mathbf{c}_p. \quad (12)$$

The control scheme we propose is based on driving the robots' current image projections  $\mathbf{p}$  to the positions  $\mathbf{p}^d$ .

### III. MULTIPLE-CAMERA COORDINATED VISUAL CONTROL

In this section, we employ the homography-based framework presented thus far to propose a coordinated control scheme of the multirobot system with multiple cameras.

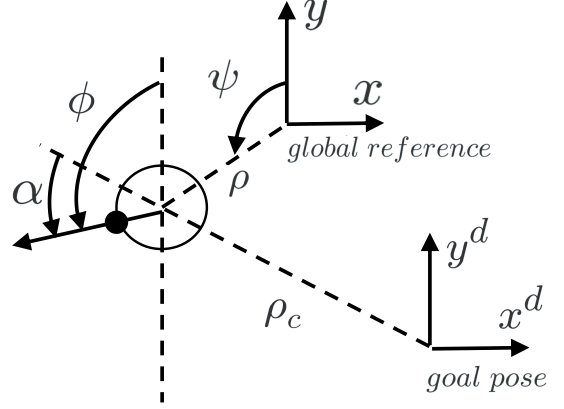


Fig. 3. Top view of the plane where the robots lie. Each robot's state is expressed as  $(x, y, \phi)^T$  or  $(\rho, \alpha, \phi)^T$  in the global reference frame. The depicted variables are described in the text.

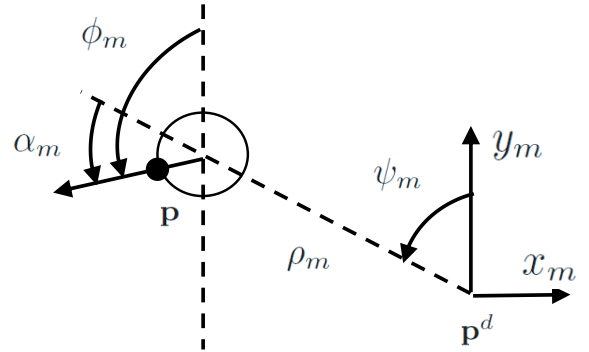


Fig. 4. Geometric variables used to control each robot, defined in the image plane. Point  $\mathbf{p}$  is the projection of a robot in the current image, and  $\mathbf{p}^d$  its desired location within the desired configuration of the robot set.

#### A. Multi-camera framework and coordinate systems

We define in this section the model of the robots to be controlled, the parameters used in our control scheme and the characteristics of the multi-camera control framework. Note that the subscripts identifying an individual generic robot will be omitted throughout this section for clarity.

Figure 3 shows the coordinate systems and geometric variables in 3D space. The localization of each robot is expressed as  $(x, y, \phi)^T$  or  $(\rho, \psi, \phi)^T$  in the global reference frame, where

$$x = -\rho \sin \psi, \quad y = \rho \cos \psi, \quad \alpha = \phi - \psi. \quad (13)$$

We assume the robots have unicycle kinematics, and are commanded through two velocity inputs: the linear velocity  $v$  in the direction of motion, and the angular velocity  $\omega$  about the axis perpendicular to the ground plane.

We depict in Fig. 4 the variables that define the state of each of the robots in the image plane, given by  $(\rho_m, \psi_m, \phi_m)^T$ . The coordinate system for robot  $\mathbf{p}$  in the image plane is centered in the desired position  $\mathbf{p}^d$ . Thus, the robot set is in the desired configuration when for every robot, its image projection is at the origin of its reference.

The distance,  $\rho_m$ , between the current projection of a robot in the image plane  $\mathbf{p}$  and its desired position  $\mathbf{p}^d$  is given by:

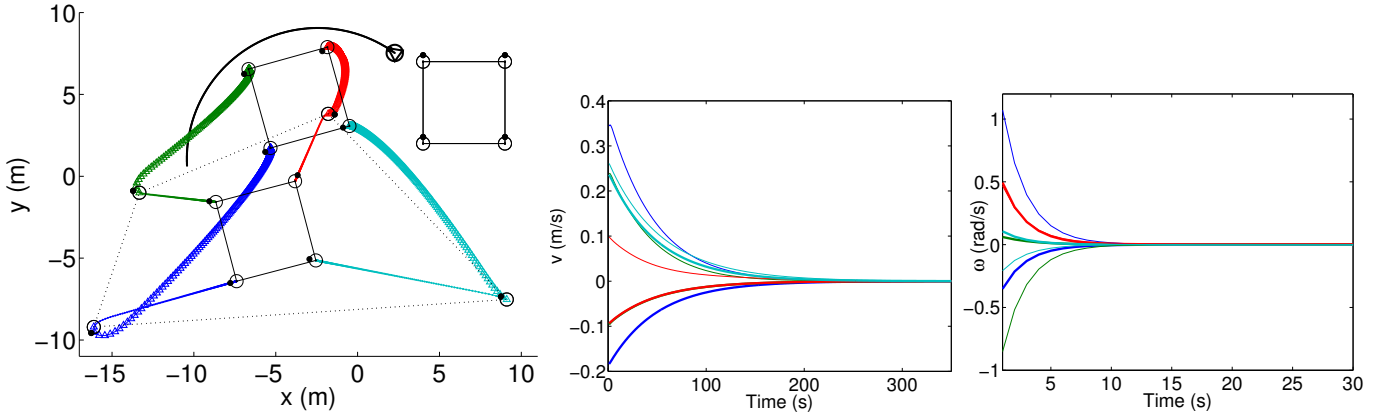


Fig. 5. Simulation results for the single-camera control method. Left: Robot paths, for the method proposed in [15] (thick lines) and the method proposed in this paper (thinner lines). The desired configuration (a square) is shown top-right of this plot. The initial positions of the robots are linked by dashed lines. The camera motion is shown, represented as a circle with an inscribed triangle. Center and right: Linear and angular velocities, respectively. The curves from the method of [15] are depicted in thin lines, while the curves of our method are plotted with thick lines.

$$\rho_m = \sqrt{(p_x - p_x^d)^2 + (p_y - p_y^d)^2}, \quad (14)$$

The angle  $\psi_m$  can be computed as:

$$\psi_m = \text{atan2}(-p_x - p_x^d, p_y - p_y^d). \quad (15)$$

We can obtain  $\phi_m$  directly from the image of the robot. The alignment error in the image,  $\alpha_m$ , can then also be obtained as  $\alpha_m = \phi_m - \psi_m$ .

Let us define next the elements of the multi-camera system. We consider a set of  $n$  mobile robots and a set of  $m$  cameras, each of which observes a subset of robots  $S_i$ ,  $i = 1, \dots, m$ . Our assumption is that for every value of  $i$ , at least two of the robots in  $S_i$  also belong to another subset (or group of subsets)  $S_j$ , with  $i \neq j$ .

Each camera has an associated control unit that issues motion commands to all the robots in its field of view (i.e. to the robots in  $S_i$ ). These commands are generated employing the homography-based control law that will be described in the following section, which is based on the desired positions determined as discussed in section II-B. Each control unit has the information of the full desired configuration defined in the image plane, but only uses at any time the part of it corresponding to the robots in  $S_i$ . The way in which each robot computes its actual control command is also discussed in the next section.

### B. Visual control law

We propose a control scheme through which a control unit can drive the set of robots within the field of view of its associated camera to the desired configuration. The scheme is based on the desired homography computed as described in section II-B. We use this homography to define, using (12), the set of desired positions  $\mathbf{p}^d$  for the robots in the image plane. Then, we propose an image-based control law to drive the projections of the robots from their current positions to the desired ones, using the variables defined in section III-A.

The linear velocity of our control for each robot is defined as proportional to the distance to the target image position,

while the angular velocity performs orientation correction to align the robot with the direction to the goal, as follows (again, we do not include a subscript for the robot for clarity):

$$\begin{cases} v = -k_v \text{sign}(\cos \alpha_m) \rho_m \\ \omega = k_\omega (\alpha_d - \alpha_m) \end{cases}, \quad (16)$$

where  $k_v > 0$  and  $k_\omega > 0$  are control gains, and the angle  $\alpha_d$  is defined as:

$$\alpha_d = \begin{cases} 0 & \text{if } |\alpha_m| \leq \frac{\pi}{2} \\ \pi & \text{if } |\alpha_m| > \frac{\pi}{2} \end{cases}.$$

With this control, each robot can travel forwards or backwards depending on its location relative to its desired position. Note that the final orientation of the robots is not controlled to a particular value. If we consider that the robots have omnidirectional capabilities, the correction of their orientation at the end of the control task is not critical.

Each of the controlled robots can receive multiple motion commands from different control units at any time. We note that it is possible for the robots to use these commands in different ways to achieve convergence of the set to the target configuration. We choose in particular a strategy where each robot selects the received command having minimum absolute linear velocity. This strategy is simple and was experimentally observed to provide good performance in terms of trajectory smoothness and convergence speed. It is trivial that if each subset shares at least two robots with the other subsets, then when all the partial desired configurations are reached, the global desired configuration must also have been reached. Due to the characteristics of our proposed control method, the commands issued by different cameras are cooperative, and their implicit coordination results in the group being driven to the global target configuration.

Notice that in order to have this cooperative behavior, it is required to use a control whose target configuration has the same geometrical center as the current set of robots. Therefore, the methods employed in our previous homography-based multirobot control works [15], [16] would not allow to perform the control with multiple cameras.

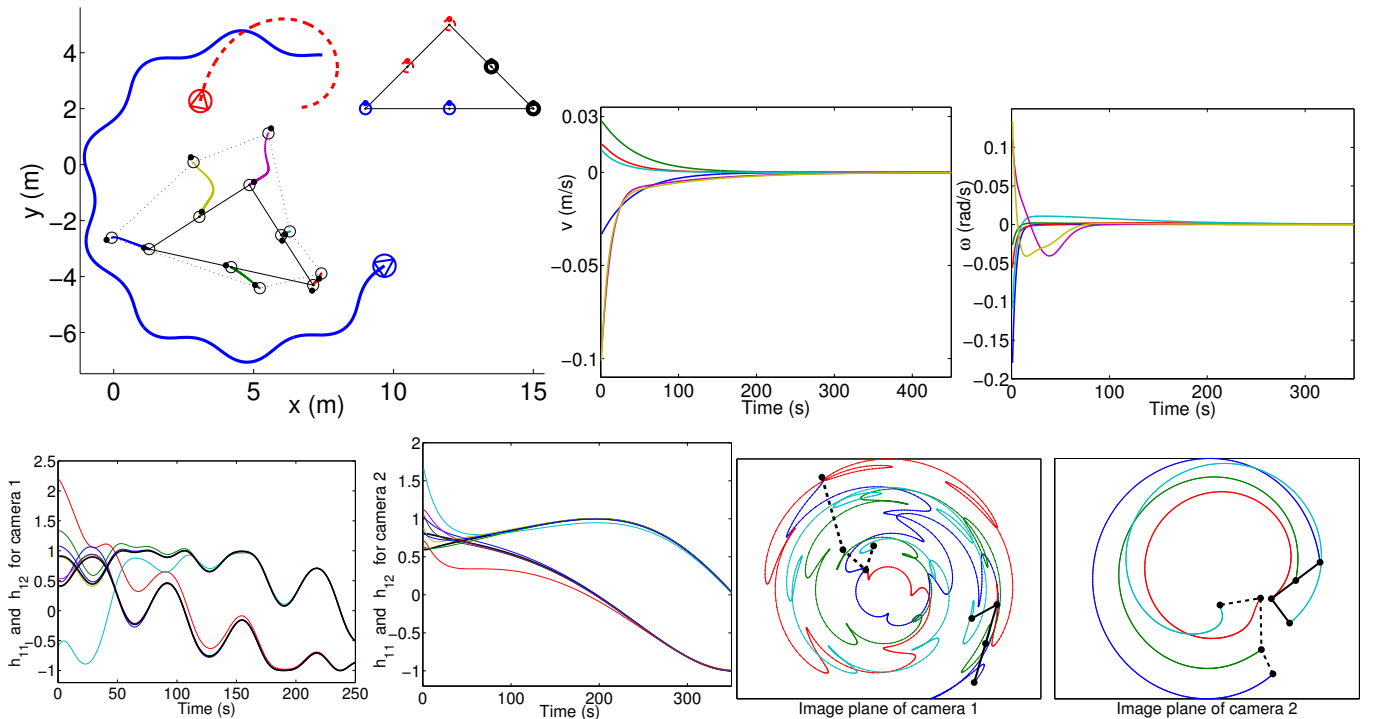


Fig. 6. Simulation results for the multi-camera control method. Top-left: Paths of the robots. The desired configuration (triangle) is shown top-right of this plot. The robots controlled only by camera 1 are shown in full lines. The robots controlled only by camera 2 are shown in dashed lines. The robots controlled by both cameras are shown in thicker full lines. The initial positions of the robots are linked by dashed lines. The motions of the cameras (represented as circles with inscribed triangles) are also shown. Camera 1 is plotted with a full line and camera 2 is plotted with a dashed line. Top-center and Top-right: Linear and angular velocities, respectively, of the robots. Bottom row-columns 1 and 2: Evolution of the homography entries for cameras 1 and 2. The elements of the desired homography computed with all the robots are displayed with a thick line, the elements of the individual homographies for each robot are displayed with thin lines. Bottom row-columns 3 and 4: Evolution of the image plane projections of the robots for cameras 1 and 2, respectively. For both plots, the initial points are displayed joined by dashed lines, while the points at the end of the control are shown joined by full lines.

### C. Stability analysis

The stability of the presented single-camera control law is analyzed next.

*Proposition 2:* The multirobot system under the control law (16) is locally exponentially stable.

*Proof:*

We define, for every robot  $i$  ( $i = 1, \dots, n$ ),  $\mathbf{x}_i(t)$  as the actual 3D position of the robot projected in the current image point  $\mathbf{p}_i(t)$ , and  $\mathbf{x}_i^d(t)$  as the actual position associated to the desired image point  $\mathbf{p}_i^d(t)$ . Let us first prove that the real positions associated to the desired image points used by our method are fixed, i.e. for  $i = 1, \dots, n$ ,  $\mathbf{x}_i^d(t)$  is constant.

Due to the definition of our homography-based framework,  $\mathbf{x}^d(t)$  are the set of desired positions for which

$$Sum(t) = \sum_{i=1}^n \|\mathbf{x}_i(t) - \mathbf{x}_i^d(t)\|^2 \quad (17)$$

is minimum. As we analyze the local stability behavior of the system, we assume that all the robots have corrected their orientation, i.e.  $\alpha_m = \alpha_d$  for each of them. Then, the control moves the robots straight to their desired positions, in such a way that  $\mathbf{x}_i(t + \delta t) = \mathbf{x}_i(t) + (\mathbf{x}_i^d(t) - \mathbf{x}_i(t)) \cdot k_s \delta t$ , where  $k_s$  is a positive constant proportional to the linear velocity gain of the control,  $k_v$ . Now, if we assume the new desired positions may have changed instantaneously, let us define

them as:  $\mathbf{x}_i^d(t + \delta t) = \mathbf{x}_i^d(t) + \Delta_i$ . We then have:

$$\begin{aligned} Sum(t + \delta t) &= \sum_{i=1}^n \|\mathbf{x}_i(t + \delta t) - \mathbf{x}_i^d(t + \delta t)\|^2 = \\ &= \sum_{i=1}^n \|\mathbf{x}_i(t) + (\mathbf{x}_i^d(t) - \mathbf{x}_i(t)) \cdot k_s \delta t - \mathbf{x}_i^d(t) - \Delta_i\|^2 = \\ &= (1 - k_s \delta t) \cdot \sum_{i=1}^n \|\mathbf{x}_i(t) - (\mathbf{x}_i^d(t) + \Delta_i / (1 - k_s \delta t))\|^2, \quad (18) \end{aligned}$$

Now, if we compare this expression with (17), it can be seen that if a given set of positions  $\mathbf{x}^d(t)$  make (17) minimum, then in order for (18) to be minimum, it must hold that  $\Delta_i = (0, 0)^T$  for  $i = 1, \dots, n$ . Thus, the real position for each robot corresponding to its desired point in the image plane remains fixed, i.e. for  $i = 1, \dots, n$ ,  $\mathbf{x}_i^d(t)$  is constant.

Given that the kinematics of each robot can be expressed as  $\dot{\rho} = v \cos \alpha$ , the distance to its fixed goal for any of the robots verifies:

$$\dot{\rho}_c = -v = -k_v \rho_m = -k_s \rho_c. \quad (19)$$

Thus, it is straightforward to see that the convergence of each robot to its fixed desired position is bounded by an exponential decay, i.e. the multirobot system is locally exponentially stable. ■

#### IV. EXPERIMENTS

Next, we provide simulation results in order to illustrate the performance of our approach. For simplicity, we used conventional cameras, having the following calibration matrix:  $K = [(640, 0, 0)^T, (0, 480, 0)^T, (320, 240, 1)^T]$ . We first present results for the control described in section III-B implemented on a single camera. In order to evaluate our approach, we consider an example of a set of four robots having to form a square-shaped desired configuration. We show the performance and compare it with the control of the previous work [15]. The results are displayed in Fig. 5. As can be observed, the proposed control generates shorter trajectories than those of the previous approach. We can see as well that the trajectories are straight lines once the robots have corrected their angular error (i.e. the desired positions remain constant). This good behavior is worthy of note considering that our method does not perform any position estimation and is purely image-based.

We show in Fig. 6 results from an example of the multiple-camera control. It can be seen that the six robots reach the desired formation (triangle) when controlled through two cameras. Each camera is used to control four robots, and two of the robots are common. Although the gains of the control were manually selected for better visualization of the results, satisfactory performance was observed for wide ranges of values for the gains. The image plane representations in the same figure illustrate the importance of the use of the homography, the tool that makes it possible to abstract, based on the image information, the motion of the robots from the camera motion. The evolution of the entries  $h_{11}$  and  $h_{12}$  of the desired homography is also displayed, along with the entries of the homographies computed from each robot individually. All the individual homographies eventually converge to the desired homography as the control moves the robots to their positions in the desired configuration.

#### V. DISCUSSION AND CONCLUSION

We have presented a homography-based multirobot control approach where multiple cameras are used to observe and control a set of robots moving on the ground plane in order to bring them to a desired configuration. The method relies on the overlap of two robots between the subsets seen by the cameras. In practice, maintaining an overlap of only one robot could be sufficient. In this case, the control we define has the effect of making the robots come closer, which would easily lead to an increase in the overlap between subsets.

The advantages of the partially distributed control approach presented with respect to a centralized method (i.e. one that uses only a single camera and controller) are that it overcomes the field of view limitation of a single camera, and it is more scalable, since the processing load of the task is shared between multiple control units. Its redundancy makes it more robust to failure as well. With respect to a purely distributed method, in our approach the robots have smaller sensing and processing requirements, and do not need to transmit any information.

The system should be dimensioned properly, in terms of the number of cameras needed. This should take into account the processing capabilities for each control unit, the field of view of each camera, the total number of robots and the size of the desired configuration, determined by the distances between robots. We believe the proposed method has potential to be developed further in different ways. Since one of the advantages of the approach is that the cameras can move arbitrarily, one objective can be to devise methods that optimize the visibility of the set of robots and guarantee that sufficient overlap between subsets will be maintained. It would also be interesting to investigate different strategies for a robot to determine its motion when it receives multiple simultaneous commands.

#### REFERENCES

- [1] J. Chen, D. Sun, J. Yang, and H. Chen, "Leader-Follower Formation Control of Multiple Non-holonomic Mobile Robots Incorporating a Receding-horizon Scheme," *The International Journal of Robotics Research*, vol. 29, no. 6, pp. 727–747, 2010.
- [2] J. Ghommam, H. Mehrjerdi, and M. Saad, "Leader-follower formation control of nonholonomic robots with fuzzy logic based approach for obstacle avoidance," in *IEEE/RSJ International Conference on Intelligent Robots and Systems*, 2011, pp. 2340–2345.
- [3] S. Zhao, S. Ramakrishnan, and M. Kumar, "Density-based control of multiple robots," in *American Control Conference*, 2011, pp. 481–486.
- [4] K. Listmann, M. Masalawala, and J. Adamy, "Consensus for formation control of nonholonomic mobile robots," in *IEEE International Conference on Robotics and Automation*, 2009, pp. 3886–3891.
- [5] Z. Kan, A. Dani, J. Shea, and W. Dixon, "Ensuring network connectivity for nonholonomic robots during rendezvous," in *IEEE Conf. on Decis. and Control and Europ. Control Conf.*, 2011, pp. 2369–2374.
- [6] A. K. Das, R. Fierro, V. Kumar, J. P. Ostrowski, J. Spletzer, and C. J. Taylor, "A vision-based formation control framework," *IEEE Trans. on Robotics and Automation*, vol. 18, no. 5, pp. 813–825, 2002.
- [7] J. Alonso-Mora, A. Breitenmoser, M. Ruffi, R. Siegwart, and P. Beardley, "Multi-robot system for artistic pattern formation," in *IEEE Int. Conf. on Robotics and Automation*, 2011, pp. 4512–4517.
- [8] R. Vidal, O. Shakernia, and S. Sastry, "Following the flock: Distributed formation control with omnidirectional vision-based motion segmentation and visual servoing," *IEEE Robotics and Automation Magazine*, vol. 11, no. 4, pp. 14–20, 2004.
- [9] N. Moshtagh, N. Michael, A. Jadbabaie, and K. Daniilidis, "Vision-based, distributed control laws for motion coordination of nonholonomic robots," *IEEE Trans. Rob.*, vol. 25, no. 4, pp. 851–860, 2009.
- [10] G. Mariottini, F. Morbidi, D. Prattichizzo, N. Vander Valk, N. Michael, G. Pappas, and K. Daniilidis, "Vision-based localization for leader-follower formation control," *IEEE Trans. Rob.*, vol. 25, no. 6, pp. 1431–1438, 2009.
- [11] F. Chaumette and S. Hutchinson, "Visual servo control, part I: Basic approaches," *IEEE Rob. Autom. Mag.*, vol. 13, no. 4, pp. 82–90, 2006.
- [12] J. Chen, W. Dixon, M. Dawson, and M. McIntyre, "Homography-based visual servo tracking control of a wheeled mobile robot," *IEEE Transactions on Robotics*, vol. 22, no. 2, pp. 407–416, 2006.
- [13] J. Courbon, Y. Mezouar, and P. Martinet, "Indoor navigation of a non-holonomic mobile robot using a visual memory," *Autonomous Robots*, vol. 25, no. 3, pp. 253–266, 2008.
- [14] G. López-Nicolás, N. R. Gans, S. Bhattacharya, J. J. Guerrero, C. Sagiés, and S. Hutchinson, "Homography-based control scheme for mobile robots with nonholonomic and field-of-view constraints," *IEEE Trans. on Sys., Man, and Cybern., Part B: Cybern.*, vol. 40, no. 4, pp. 1115–1127, 2010.
- [15] G. López-Nicolás, Y. Mezouar, and C. Sagiés, "Homography-based multi-robot control with a flying camera," in *IEEE International Conference on Robotics and Automation*, 2011, pp. 4492–4497.
- [16] G. López-Nicolás, M. Aranda, Y. Mezouar, and C. Sagiés, "Visual control for multirobot organized rendezvous," *IEEE Trans. Sys., Man, and Cybern., Part B: Cybern.*, vol. 42, no. 4, pp. 1155–1168, 2012.